Order Parameter for the Transition from Phase to Amplitude Turbulence

Alessandro Torcini
Theoretical Physics, Wuppertal University, D-42097 Wuppertal, Germany
(Received 15 April 1996)

The maximal conserved phase gradient is introduced as an order parameter to characterize the transition from phase to defect turbulence in the complex Ginzburg-Landau equation. It has a finite value in the phase-turbulent regime and decreases to zero when the transition to defect turbulence is approached. Solutions with a nonzero phase gradient are studied via a Lyapunov analysis. The degree of "chaoticity" decreases for increasing values of the phase gradient and finally leads to stable traveling wave solutions. A modified Kuramoto-Sivashinsky equation for the phase dynamics is able to reproduce the main features of the stable waves and to explain their origin. [S0031-9007(96)00860-5]

PACS numbers: 47.27.Cn, 05.45.+b, 47.27.Eq

Spatially extended chaotic systems have been recently the subject of several theoretical and experimental investigations [1]. In spite of remarkable progress, a still unresolved problem concerns the possibility to describe nonequilibrium phase transitions with concepts borrowed from statistical mechanics [1–4]. The complex Ginzburg-Landau equation (CGLE) is one of the most appropriate models to study such transitions, because it is universal [1,5] and experimentally relevant [6]: the dynamics of extended systems undergoing a Hopf bifurcation from a stationary to an oscillatory state is described by the CGLE [7]. Moreover, several physical, chemical, and biological phenomena can be well reproduced through the CGLE [1]. Even in one dimension the CGLE displays a variety of dynamical regimes and phase transitions [2–4,7–9]. Among them much attention has been devoted to the transition between two different types of chaotic phases [2–4,7,8]: namely, the phase-turbulent (PT) and defect-turbulent (DT) regimes. However, this transition has been mainly studied from the DT side [2–4].

This Letter focuses on the PT regime and in particular on the introduction of an order parameter for the above mentioned transition. To be more specific, let me write the one-dimensional CGLE as

$$A_t = (1 + ic_1)A_{xx} + A - (1 - ic_3)\,|A|^2 A\,, \qquad (1)$$

where the parameters c_1 and c_3 are real positive numbers, and $A(x,t) = \rho(x,t)\exp[i\psi(x,t)]$ is a complex field of amplitude ρ and phase ψ. Of particular interest in the (c_1, c_3) plane is the so-called Benjamin-Feir line (BFL) defined by $c_3 = 1/c_1$, which identifies the linear stability limit for the plane-wave solutions of (1) [5]. The PT regime is encountered just above the BFL (i.e., for $c_3 > 1/c_1$) [7]. In this state the chaotic behavior of the field is essentially ruled by the dynamics of the phase. Moreover, the amplitude is always bounded away from zero, accordingly; the average phase gradient $\nu = \frac{1}{L}\int_0^L dx\, \partial_x \psi(x,t)$ is conserved for periodic boundary conditions [7]. Another important line (L_1) separates the PT state from a more chaotic phase: the DT regime. In this state, amplitude dynamics becomes predominant over phase dynamics [2,7,8]. In particular, large amplitude oscillations are observed, occasionally driving $\rho(x,t)$ to zero, in which case the phase is no longer well defined and ν is not conserved. The vanishing of the amplitude determines a so-called space-time defect. The density of defects δ_D is a good order parameter to characterize the transition from the DT to the PT phase; in fact, its value is >0 in the DT regime, while it vanishes approaching the PT phase [2,4]. Conversely, none of the other parameters introduced so far (e.g., phase and amplitude correlations lengths, or the Kaplan-Yorke dimension density) reveals a clear signature of the transition [3,4].

In the PT regime, a relevant parameter to characterize a state of the CGLE is the value of ν, which is a conserved quantity in the absence of defects. For each value of $\nu < 1$ there exists a plane-wave solution of the CGLE

$$A(x,t) = \sqrt{1 - \nu^2}\exp[i(\nu x + \Omega_0 t)], \qquad (2)$$

where $\Omega_0 = c_3 - (c_1 + c_3)\nu^2$. Below the BFL, these solutions are stable against long-wavelength instabilities for $\nu^2 < (1 - c_1c_3)/[2(1 + c_3^2) + 1 - c_1c_3]$ [5], while they turn out to be all unstable in the PT regime. However, it is reasonable to expect that different ν values will characterize distinct classes of chaotic or quasiperiodic solutions also in the PT phase. Nevertheless, the majority of analyses reported in literature has been devoted to solutions with $\nu = 0$.

In this Letter, I determine the maximal value ν_M of the conserved phase gradient in statistically stationary states, i.e., in the limit $L \to \infty$ and $t \to \infty$. I shall argue that this can be used as an order parameter, with $\nu_M = 0$ in the DT regime, with $\nu_M > 0$ in the PT state, and with a smooth change at the transition line L_1. Moreover, a Lyapunov analysis reveals that for increasing ν values the solutions are less and less chaotic. This behavior can be explained assuming that the phase dynamics is ruled by a modified Kuramoto-Sivashinsky equation (MKSE) [7,10–12]. For reasonably high ν values traveling pulse-train solutions are found to be stable. The main parameters characterizing such solutions can be derived from the above mentioned MKSE.

The analysis reported here is limited to a parameter region where it is known that the CGLE shows a continuous transition from the PT to the DT regime [2,4], namely, $c_1 = 3.5$ and $c_3 \geq 1/c_1$. The integration scheme adopted here is a time splitting code where the integration of the spatial derivatives is not performed, as usual, in Fourier space, but instead is computed in x space through a convolution integral [13,14]. The adopted integration parameters are spatial resolution $dx = 0.5$, integration time step $dt = 0.05$, number of grid points $N = L/dx$ ranging from 2048 up to 8192, and periodic boundary conditions.

In order to study solutions with a nonzero value of ν, an initial state with $\nu \neq 0$ has been prepared and its evolution followed. Because of the absence of defects in the PT regime, ν should be conserved, at least for small initial values. I have numerically verified that ν is indeed conserved for all values below an upper limit ν_M. For $\nu > \nu_M$ defects eventually arise leading, after a readjusting time, to a ν value smaller than ν_M. This behavior can be understood by observing that the minimal ρ value decreases continuously for increasing ν, until, for $\nu > \nu_M$, the amplitude can eventually vanish with the consequent emergence of defects. In order to evaluate the maximal phase gradient accurately, the conservation of each ν_M value reported in Fig. 1 has been checked considering from 50 to 70 different initial conditions. In particular, each configuration has been followed for a time $t \geq 10\,000$, after a reasonably long transient had been discarded. Moreover, for each examined c_3 value, some trajectories have been followed for longer times, typically of the order of $t = 150\,000$. No dependence of ν_M on L has been observed, considering chain lengths from $L = 1024$ up to $L = 4096$. Figure 1 shows a roughly linear decrease of ν_M for increasing values of c_3. A linear fit of the data gives $\nu_M \simeq -0.74c_3 + 0.57$. Assuming that the linear behavior extends up to the L_1 line, a critical value $c_3^* = 0.76 \pm 0.03$ is obtained. This result is in reasonable agreement with the values obtained from the defect density reported in literature [2,4], as well as with our own measurements of δ_D, which give $c_3^* = 0.755 \pm 0.002$ [13,15].

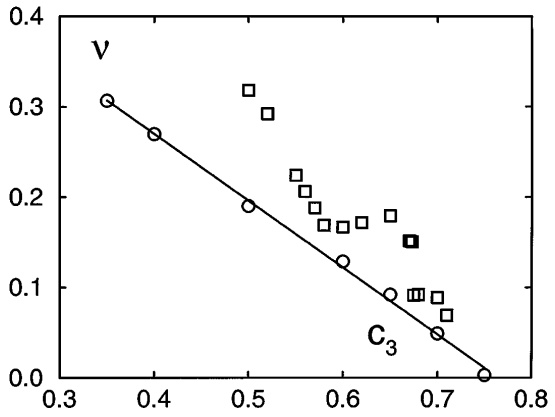

FIG. 1. Maximal phase gradient ν_M as a function of the parameter c_3 (circle). The values for ν_U are also shown (squares). The solid line represents a linear fit for the ν_M data.

As a further characterization of these solutions, I have evaluated the maximal Lyapunov exponent λ_M for several values of c_3 and ν. I noticed multistability for $\nu > 0$, i.e., several coexisting attractors for each ν value, different attractors being characterized by different Lyapunov exponents. However, a characteristic common to all these initial conditions considered is that λ_M tends to decrease with increasing ν, except for small fluctuations (see Fig. 2). In particular, for $c_3 \leq 0.5$ and for sufficiently high values of ν, nonchaotic states are found. Two different kinds of nonchaotic states have been observed: the former (type α) is spatially periodic with spatial wave vector $q = \nu$, formed of identical "pulselike" structure of length $L_P = 2\pi/\nu$; the latter (type β) shows essentially periodic regions separated by domains in which ρ is constant and the phase decreases linearly (see Fig. 3). The selection of these patterns depends on the initial conditions. Numerically I found that all nonchaotic solutions are of the form

$$A(x,t) = h(x - vt)e^{i(\nu x + \omega t)}, \tag{3}$$

where $h(\xi) = \rho(\xi)\exp[i\psi_0(\xi)]$ is in general complex. Amplitude and phase can be written as

$$\rho(x,t) = \rho(\xi), \quad \psi(x,t) = \psi_0(\xi) + \omega t + \nu x, \tag{4}$$

with $\xi = x - vt$.

For spatially periodic patterns, the elementary pulses of length L_P are a stable solution of the CGLE for a short

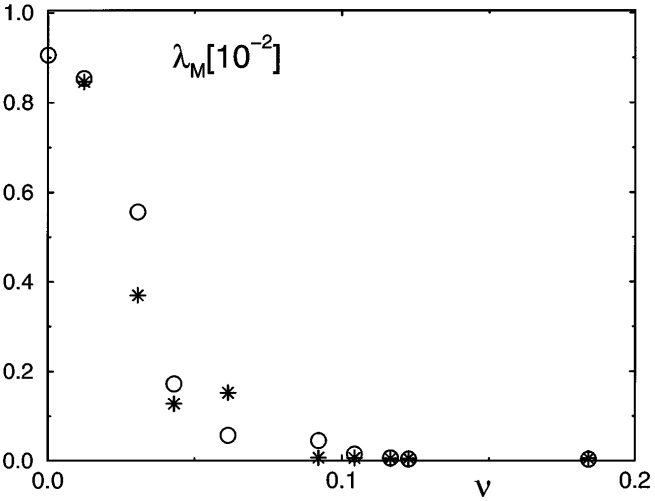

FIG. 2. Maximal Lyapunov exponents versus the phase gradient ν for two different sets of initial conditions for $c_3 = 0.5$. The two initial conditions correspond to states with phase gradient ν and with noise added only on the amplitude (circle) or added on both amplitude and phase (asterisks). The data have been obtained for system size $L = 1024$ and for integration times $t = 130\,000-250\,000$.

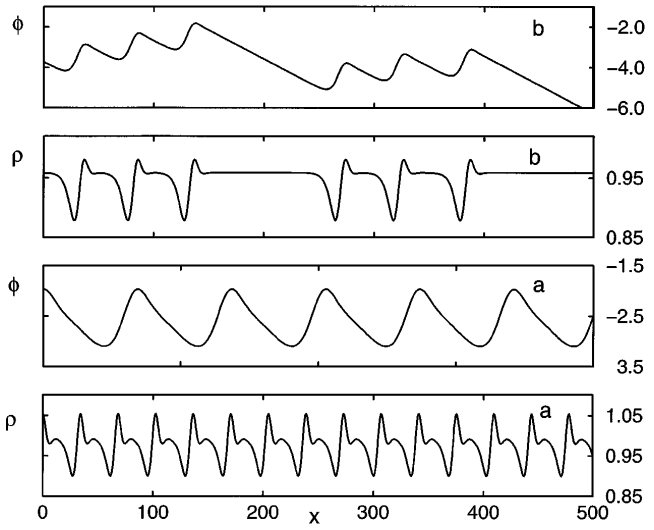

FIG. 3. Phase and amplitude for the two kinds of observed nonchaotic solutions: (a) solution of type α with $c_3 = 0.5$ and $\nu = 0.184$; (b) solution of type β with $c_3 = 0.35$ and $\nu = 0.307$.

chain of length $L = L_P$ and with a phase gradient $\nu_P = 2\pi/L_P$, i.e., the minimal nonvanishing phase gradient for such a periodic system. These traveling pulses originate through a bifurcation from the plane-wave solutions (2). Moreover, they are stabilized in short systems, because of the long-wavelength instability cutoff. A more extensive and detailed study of these short-chain solutions will be reported elsewhere. Here, I want just to point out that solutions with a conserved ν_P are no longer observable below a minimal length $L_{\min}$. The corresponding phase gradient $\nu_U = 2\pi/L_{\min}$ is an upper bound for ν_M, as shown in Fig. 1. For increasing c_3, the value ν_M is better and better approximated by ν_U. A naive explanation of this fact can be given by assuming that, in the proximity of ν_M, only stable solutions of type α are observed. For these solutions the minimal value of the spatial period is obviously $L_{\min}$ and the maximal possible phase gradient ν_U. However, in the limit $\nu \to \nu_M$, for $c_3 \leq 0.5$ solutions of type α coexist with those of type β, while for $c_3 > 0.5$ slightly chaotic solutions, formed by an array of elementary pulses of different lengths $L_p \geq L_{\min}$, are observed. All these facts imply that $\nu_U \geq \nu_M$.

As a final point, I explain why λ_M decreases with increasing ν. This can be done by recalling that just above BFL the dynamics is essentially ruled by the phase behavior, since the amplitude can be considered as a "slaved" variable of the phase [7,8,12]. A phase modulation $\phi(x,t) = \psi(x,t) - \nu x = \psi_0(\xi) + \omega t$ on the plane-wave solution (2) satisfies a MKSE [11],

$$\dot{\phi} - \Omega_0 + \Omega_1 \partial_x \phi + \Omega_2^{(1)} \partial_x^2 \phi + \Omega_2^{(2)} (\partial_x \phi)^2 + \Omega_3 \partial_x^3 \phi + \Omega_4^{(1)} \partial_x^4 \phi + \Omega_4^{(2)} \partial_x \phi \, \partial_x^3 \phi = 0, \quad (5)$$

where $\Omega_1 = 2\nu(c_1 + c_3)$, $\Omega_2^{(1)} = c_1 c_3 - 1$, $\Omega_2^{(2)} = c_1 + c_3$, $\Omega_3 = 2\nu c_1 (1 + c_3^2)$, $\Omega_4^{(1)} = c_1^2 (1 + c_3^2)/2$, and $\Omega_4^{(2)} = 2c_1(1 + c_3^2)$. In order to check the validity of Eq. (5) for the dynamics of the phase for the CGLE in the PT regime, I derive from Eq. (5) an expression for the velocity v and the frequency ω of the traveling solutions (3). Following [11], I obtain

$$\omega = \Omega_0 - \Omega_2^{(2)} \langle (\partial_\xi \psi_0)^2 \rangle + \Omega_4^{(2)} \langle (\partial_\xi^2 \psi_0)^2 \rangle \quad (6)$$

$$v = \Omega_1 + [\Omega_2^{(2)} \langle (\partial_\xi \psi_0)^3 \rangle - \Omega_3 \langle (\partial_\xi^2 \psi_0)^2 \rangle + \Omega_4^{(2)} \langle (\partial_\xi \psi_0)^2 \partial_\xi^3 \psi_0 \rangle] / \langle (\partial_\xi \psi_0)^2 \rangle, \quad (7)$$

where $\langle \cdot \rangle$ is the average along the chain and over several consecutive realizations. The two expressions can easily be obtained by noticing that for a solution of type (4) the temporal derivative of the phase can be written as $\dot{\phi} = \omega - v \partial_\xi \psi_0(\xi)$, while $\partial_x \phi(x) = \partial_\xi \psi_0(\xi)$. Substituting the temporal derivative into Eq. (5) and averaging both sides of the equation leads to Eq. (6). To obtain Eq. (7) both sides of Eq. (5) should be multiplied by $\partial_\xi \psi_0(\xi)$ before averaging. Several quantities appearing in Eq. (5) have zero average due to the periodic boundary conditions. Therefore the final expressions for ω and v are drastically simplified. By inserting the phase values obtained from simulations of the CGLE into Eqs. (6) and (7), a very good agreement with the measured quantities is indeed achieved (see Table I). Nevertheless, I expect that the phase description (5) will become less and less accurate approaching the L_1 line and will finally break down when the amplitude dynamics becomes predominant. However, I have verified that in the whole examined parameter interval the amplitude dynamics is essentially ruled by the phase, except when defects arise.

Assuming that Eq. (5) describes sufficiently well the dynamics of the CGLE phase, let me now explain

TABLE I. The parameters characterizing the stable solutions (3), namely, the propagation velocity v and the frequency ω, are reported for various ν values. The values are estimated using expressions (6) and (7). In parentheses are the values measured directly from the traveling waves solutions. All data refer to $c_3 = 0.5$, except where noted.

ν	ω	v	ν	ω	v
0.123	0.428 (0.427)	1.26 (1.24)	0.123[a]	0.428 (0.424)	1.06 (1.09)
0.184	0.355 (0.341)	1.59 (1.65)	0.184[a]	0.344 (0.338)	1.58 (1.63)
0.245	0.229 (0.223)	1.93 (1.98)	0.282[b]	0.074 (0.070)	2.37 (2.34)

[a]Solutions corresponding to different initial conditions, but with the same ν.
[b]Data where $c_3 = 0.4$.

the observed nonchaotic behaviors. In Ref. [11] it has been shown that Eq. (5), rewritten for the variable $\partial_x \phi$, belongs to a class of equations that shows stable solutions formed by pulselike periodic structures traveling along the chain with a finite velocity [16,17]. The birth of these nonchaotic solutions is due to the presence of the dispersion term $\propto \partial_x^3 \phi$ [16]. In particular, in Ref. [17] it has been shown that this equation is multistable: chaotic and nonchaotic solutions can coexist. However, stationary periodic attractors prevail over the strange ones for increasing values of the dispersion constant Ω_3 and, above a threshold value, only nonchaotic solutions are observed. Since Ω_3 is proportional to ν, this explains the decreasing behavior of λ_M for increasing ν, as well as the origin of the observed traveling wave solutions for high ν values. Finally, it should be mentioned that for $c_3 > 0.5$ it is no longer possible to observe stable solutions, because they would occur for the value of $\nu > \nu_M$.

In conclusion, I emphasize that ν_M turns out to be a good order parameter to describe the transition from the PT to the DT phase. The role of this new parameter is complementary to that of the defect density, since it is nonzero in the PT regime, while the defect density is nonzero in the DT state. Moreover, the dynamics in the PT phase depends strongly on the ν value: for $\nu \to 0$ a predominance of chaotic solutions is observed, while for $\nu \to \nu_M$ nonchaotic behaviors prevail and a new family of stationary solutions emerges.

I am indebted to P. Grassberger for extremely effective suggestions. I thank H. Frauenkron, S. Lepri, and A. Politi for helpful discussions. Support from the European Community under Grant No. ERBCHBICT941569 and from the Cooperativa Fontenuova are also gratefully aknowledged.

[1] For a review on the subject, see M. C. Cross and P. C. Hohenberg, Rev. Mod. Phys. **65**, 851 (1993).

[2] B. I. Shraiman *et al.*, Physica (Amsterdam) **57D**, 241 (1992).

[3] D. A. Egolf and H. S. Greenside, Nature (London) **369**, 129 (1994); T. Bohr, E. Bosch, and W. van de Water, Nature (London) **372**, 48 (1994).

[4] D. A. Egolf and H. S. Greenside, Phys. Rev. Lett. **74**, 1751 (1995).

[5] P. Mannneville, *Dissipative Structures and Weak Turbulence* (Academic Press, San Diego, 1990).

[6] B. Janiaud *et al.*, Physica (Amsterdam) **55D**, 269 (1992); L. Ning and R. E. Ecke, Phys. Rev. E **47**, 3326 (1993); P. Kolodner *et al.*, Physica (Amsterdam) **85D**, 165 (1995).

[7] Y. Kuramoto, Prog. Theor. Phys. Suppl. **64**, 346 (1978).

[8] H. Sakaguchi, Prog. Theor. Phys. **84**, 792 (1990).

[9] H. Chaté, Nonlinearity **7**, 185 (1994).

[10] G. I. Sivashinsky, Acta Astronaut. **4**, 1177 (1977).

[11] H. Sakaguchi, Prog. Theor. Phys. **83**, 169 (1990).

[12] H. Sakaguchi, Prog. Theor. Phys. **85**, 417 (1991).

[13] A. Torcini, H. Frauenkron, and P. Grassberger, "A Novel Integration Scheme for Partial Differential Equations: an Application to the Complex Ginzburg-Landau Equation" (to be published).

[14] It should be noticed that this new algorithm has a numerical accuracy comparable with spectral codes, but the CPU time required for each time step is substantially reduced. The CPU time needed for this new algorithm to perform a single time step is smaller than that required for a fast-Fourier transform code by a factor $\simeq 1/\ln(N)$. In my applications, this factor was $\simeq 0.3$. For more details see [13].

[15] The defect densities δ_D have been measured on the amplitude-turbulent side for several c_3 values, in proximity of the L_1 line, and then extrapolated to zero, assuming a power-law decay $\delta_D \propto (c_3 - c_3^*)^\alpha$. From our own measurements $\alpha \simeq 3.2$, in reasonable agreement with the value reported in [2], but roughly half the estimate in Ref. [4]. For these measurements, system sizes from $L = 1024$ up to $L = 4096$ and integration times up $t = 245\,000$ have been used.

[16] T. Kawahara, Phys. Rev. Lett. **51**, 381 (1983); S. Toh and T. Kawahara, J. Phys. Soc. Jpn. **54**, 1257 (1985).

[17] H.-C. Chang, E. A. Demekhin, and D. I. Kopelevich, Physica (Amsterdam) **63D**, 299 (1993).